

Synthesis of Cu_3BiS_3 Thin Films by Heating Metal and Metal Sulfide Precursor Films under Hydrogen Sulfide

Nathan J. Gerein and Joel A. Haber*

Department of Chemistry, University of Alberta, Edmonton, Alberta, T6G 2G2 Canada

Received June 22, 2006. Revised Manuscript Received October 10, 2006

The synthesis of Cu_3BiS_3 thin films on fused silica substrates by heating Cu–Bi metal precursor films and Cu–S–Bi metal sulfide precursor films in a H_2S atmosphere has been investigated. We have systematically evaluated the effect of precursor composition and structure, heating temperature, heating profile, and gas composition and pressure. Phase-pure Cu_3BiS_3 films 250–1000 nm thick were formed, with the morphology of the resulting films being highly dependent on the composition, structure, and heating profile of the precursor films. It was found that precursor composition determines the reaction pathway, and that the reaction pathway is the dominant factor in controlling the morphology of the Cu_3BiS_3 thin film. This precursor/pathway/morphology relationship results in Cu_3BiS_3 thin films that are discontinuous or contain hollow pockets between the film and substrate, regardless of the processing conditions employed. The electrical resistivity of these Cu_3BiS_3 films ranged from 3–200 Ω cm.

Introduction

Thin film photovoltaic devices based on $\text{Cu}(\text{In,Ga})\text{Se}_2$ (CIGS) and CdTe have been commercialized and are currently realizing significant market growth. Although significant growth potential for these materials still exists, it has been reported that the availability of tellurium and indium will ultimately limit the electricity generating capacity of these devices to 4% of current global demand for CdTe and 1% for CIGS.¹ Consequently, for large-scale deployment of thin film photovoltaics, the development of new semiconductors and device configurations is required. Known sulfide minerals, many of which have semiconducting properties, provide a likely starting point for finding alternatives to CIGS and CdTe .² One such mineral, Cu_3BiS_3 , has been synthesized by the solid-state reaction of chemical-bath-deposited CuS and thermally evaporated Bi films and has been reported to have suitable optical and electrical properties for use as a PV solar absorber layer.³ Bismuth is nontoxic and has been employed in areas where toxicity is a concern, including in pharmaceuticals and as a replacement for lead in ammunition and solders.⁴ Bismuth is also relatively available, compared to indium; the U.S Geological Survey lists current global reserves of bismuth at 330 000 metric tons, whereas current global indium reserves are only 2500 metric tons.⁴

Physical vapor deposition (PVD) syntheses are compatible with existing technologies and large-scale manufacturing, and

it is expected that the development of PVD syntheses for Cu_3BiS_3 and other new materials will facilitate their utilization in photovoltaic devices. Two-step processes are often employed to synthesize chalcogenide thin films, involving the deposition of a precursor film that is subsequently heated under a reactive gas to form the target compound. For the synthesis of chalcogenide thin films, the reactive gas can be either a hydride gas or elemental vapor. In our synthesis for Cu_3BiS_3 , we have employed H_2S as the sulfur source. The utility of this approach has been demonstrated by the synthesis of device-quality films of CuInS_2 , CuInSe_2 , and $\text{CuIn}(\text{S,Se})_2$ by heating precursors in H_2S ,^{5–10} H_2Se ,^{10–12} or $\text{H}_2\text{S}/\text{H}_2\text{Se}$,¹³ respectively. Heating of $\text{Cu}(\text{In,Ga})\text{Se}_2$ in an $\text{H}_2\text{S}/\text{H}_2\text{Se}$ atmosphere has also been used to produce graded absorber layers of $\text{Cu}(\text{In,Ga})(\text{S,Se})_2$.¹⁴ In addition to the successful application of this two-step process to CIGS, the synthesis of numerous other sulfide thin films, including Ag_3SbS_3 ,¹⁵ SnS ,^{16,17} In_2S_3 ,¹⁸ and FeS_2 ,¹⁹ has also been achieved.

- (5) Dzionk, C.; Metzner, H.; Hessler, S.; Mahnke, H.-E. *Thin Solid Films* **1997**, 299, 38–44.
- (6) Gossila, M.; Mahnke, H.-E.; Metzner, H. *Thin Solid Films* **2000**, 361–362, 56–60.
- (7) Antony, A.; Asha, A. S.; Yoosuf, R.; Manoj, R.; Jayaraj, M. K. *Sol. Energy Mater. Sol. Cells* **2004**, 81, 407–417.
- (8) Binsma, J. J. M.; Van, der Linden, H. A. *Thin Solid Films* **1982**, 97, 237–243.
- (9) Watanabe, T.; Nakazawa, H.; Matsui, M. *Jpn. J. Appl. Phys., Part 2* **1999**, 38, L430–L432.
- (10) Lokhande, C. D.; Hodes, G. *Sol. Cells* **1987**, 21, 215–224.
- (11) Yüksel, Ö. F.; Başol, B. M.; Şafak, H.; Karabiyik, H. *Appl. Phys. A: Mater. Sci. Process.* **2001**, 73, 387–389.
- (12) Alberts, V. *Jpn. J. Appl. Phys., Part 1* **2002**, 41, 518–523.
- (13) Bekker, J.; Alberts, V.; Leitch, A. W. R.; Botha, J. R. *Thin Solid Films* **2003**, 431–432, 116–121.
- (14) Singh, U. P.; Shafarman, W. N.; Birkmire, R. W. *Sol. Energy Mater. Sol. Cells* **2006**, 90, 623–630.
- (15) Laubis, C.; Henrion, W.; Beier, J.; Dittrich, H.; Lux-Steiner, M. Ch. In *Thin Film Growth and Characterization*: Institute of Physics Conference Series 152; Taylor & Francis: Oxford, UK, 1998; Sect. B, pp 289–292.
- (16) Botero, M.; Cifuentes, C.; Romero, E.; Clavijo, J.; Gordillo, G. In *Proceedings of the IEEE 4th World Conference on Photovoltaic Energy Conversion*, Waikoloa, HI, May 7–12, 2006, in Press.

* Corresponding author. E-mail: joel.haber@ualberta.ca.

- (1) Andersson, B. A. *Prog. Photovolt.* **2000**, 8, 61–76.
- (2) Dittrich, H.; Vaughan, D. J.; Patrick, R. A. D.; Graeser, S.; Lux-Steiner, M.; Kunst, R.; Lincot, D. In *Proceedings of the 13th European Photovoltaic Solar Energy Conference*, Nice, France, 1995; pp 1299–1302.
- (3) Estrella, V.; Nair, M. T. S.; Nair, P. K. *Semicond. Sci. Technol.* **2003**, 18, 190–194.
- (4) George, M. W. *Mineral Commodity Summaries*; U.S. Geological Survey Report; U.S. Government Printing Office: Washington, DC, 2005.

We have evaluated the applicability of this method to the synthesis of Cu_3BiS_3 thin films by heating Cu–Bi metal precursor films and Cu–S–Bi metal sulfide precursor films, sputter deposited on fused silica substrates, in a H_2S atmosphere. Our evaluation included the systematic study of precursor composition and preparation, heating temperature, heating profile, and gas composition and pressure. Because we are presenting Cu_3BiS_3 as a novel PV material, it was necessary to limit substrate choices to those that are transparent and nonconductive and would enable us to measure the optical and electrical properties of the deposited films. Phase-pure Cu_3BiS_3 films were formed, with the morphology of the resulting films being highly dependent on the composition, structure, and heating of the precursor films. It was found that precursor composition determines the reaction pathway, and that the reaction pathway is the dominant factor in controlling the morphology of the Cu_3BiS_3 thin film. Processing conditions were optimized; however, the overriding influence of the precursor/pathway/morphology relationship results in Cu_3BiS_3 thin films that are discontinuous or contain hollow pockets between the film and substrate. On the basis of these results, we have subsequently developed a one-step reactive deposition that overcomes the limitations of the two-step process for the synthesis of Cu_3BiS_3 and produces films with morphology suitable for application in PV devices. Details of this reactive deposition are reported in a companion paper.²⁰ In this paper, we report details on the synthesis and characterization of Cu_3BiS_3 thin films by heating metal and metal sulfide precursors in the presence of H_2S , as well as the relationship between precursor composition and preparation, reaction pathway, and film morphology.

Experimental Section

Cu–Bi metal precursor films were sputtered onto fused silica substrates (50 mm \times 50 mm). Soda-lime glass substrates were also tested, but resulted in poor adhesion of as-deposited and annealed films, and produced film morphologies considerably worse than what was achieved with fused silica substrates (see the Supporting Information, Figure S1). Substrates were cleaned by immersing in 2-propanol in an ultrasonic bath for 30 min, followed by drying with a stream of N_2 . To ensure residual contamination was not the cause of poor morphology, we cleaned some substrates in 2-propanol as above; they were then immersed for 30 min in a 1:3 mixture of H_2O_2 : H_2SO_4 , rinsed with distilled H_2O , rinsed with 2-propanol, and dried with a stream of N_2 .

Precursor films were deposited employing either codeposition or multilayer deposition. Cu and Bi were DC sputtered from 3 in. diameter targets at 84 and 20 W, respectively, at an Ar pressure of 5 mTorr. During deposition, the platen was continuously rotated at 6 rpm. Under these conditions, a Cu to Bi ratio of 3:1 is obtained with equal sputtering times. Sputter rates were calibrated by mass/area, and the stoichiometry of cosputtered films was determined by wavelength dispersive X-ray spectroscopy (WDX). Net binary film thicknesses ranged from approximately 250 to 1000 nm.

Multilayer thin films were built of elemental layers approximately 125 nm thick, starting with Cu and ending with Bi. The alternate stacking sequence was tested, with no significant impact on Cu_3BiS_3 film quality. Studies on the selenization of Cu–In metal precursors under H_2Se have also found that the stacking sequence of multilayer precursors does not have a significant effect.²¹ Cu and Bi elemental precursor films were deposited at the same powers employed for binary films and were approximately 500 nm thick.

Cu–S–Bi metal sulfide precursors were also deposited on fused silica substrates, cleaned in the same manner as outlined above. The CuS target was sputtered continuously at 80 W RF. The Bi target was sputtered at 10 W DC and cycled on and off to achieve the required stoichiometry. Targets were 3 in. in diameter, the platen was rotated at 6 rpm, and the sputtering gas was Ar at a pressure of 5 mTorr. Stoichiometry of homogeneous thin films (Cu–S or Cu–Bi–S) was determined by WDX analysis. The correct elemental ratio of Cu:Bi (following heating under H_2S) was achieved by cosputtering for 9 min, followed by 41 min of sputtering the CuS target only. Each 50 min cycle produced approximately 130 nm of deposition and was repeated six times to produce films with a final thickness of approximately 800 nm.

All precursor films were processed by heating in a H_2S atmosphere. The 40 L evacuated reaction chamber ($\sim 1 \times 10^{-6}$ Torr base pressure) was backfilled with 50 Torr H_2S , 5 Torr $\text{H}_2\text{S}/45$ Torr Ar, 5 Torr $\text{H}_2\text{S}/5$ Torr Ar, or 1 Torr $\text{H}_2\text{S}/9$ Torr Ar, yielding total chamber pressures of 50 or 10 Torr. Heating was controlled with a programmable resistance heater. Precursor films were processed for 2–30 h at temperatures ranging from 175 to 400 °C; heating rates were varied from 2 to 20 °C/min, with the cooling rate fixed at 2 °C/min.

Product thin films were characterized using scanning electron microscopy/energy dispersive X-ray spectroscopy (SEM/EDX) (JEOL 6031F SEM, Hitachi S-4800 FESEM, Hitachi S3000N VPSEM), WDX (JEOL 8900 microprobe), and X-ray diffraction (XRD) (Bruker D8 diffractometer with area detector). Sheet and electrical resistivities of the product films were measured using the van der Pauw method²² (square 2.5 cm \times 2.5 cm sample, test leads attached with 1 mm silver print contacts on each edge, Keithley 2400 source/measure unit). The van der Pauw method was selected because the use of larger silver print contacts, relative to a 4-point probe, enables reliable and reproducible contacts to be made to films with voids. Four-point probe measurements were also tried, but the non-reproducible contacts that resulted were reflected in the reproducibility of the data. Optical transmission data was also collected (Perkin-Elmer spectrophotometer); however, as a consequence of film morphology and resulting scattering losses, optical data could not be used to quantitatively assess the optical properties of the films.

Results

Heating of both metal and metal sulfide precursor films in the presence of H_2S resulted in the synthesis of phase-pure Cu_3BiS_3 ; however, the morphology of the product films was highly dependent on precursor composition and heating conditions. Cosputtered metal precursors were smooth, continuous, and mirrorlike in appearance, with insufficient surface topography to produce meaningful contrast in SEM images. Multilayer metal precursors exhibited increased

(17) Reddy, K. T. R.; Reddy, P. P.; Datta, P. K.; Miles, R. W. *Thin Solid Films* **2002**, *403*–404, 116–119.

(18) Yoosuf, R.; Jayaraj, M. K. *Sol. Energy Mater. Sol. Cells* **2005**, *89*, 85–94.

(19) Pimenta, G.; Kautek, W. *Thin Solid Films* **1994**, *238*, 213–217.

(20) Gerein, N. J.; Haber, J. A. *Chem. Mater.* **2006**, *18*, 6297–6302.

(21) Alberts, V.; Swanepoel, R. *J. Mater. Sci.: Mater. Electron.* **1996**, *7*, 91–99.

(22) Schroder, D. K. *Resistivity*. In *Semiconductor Material and Device Characterization*, 2nd ed.; John Wiley and Sons, Inc.: New York, 1998; pp 2–17.

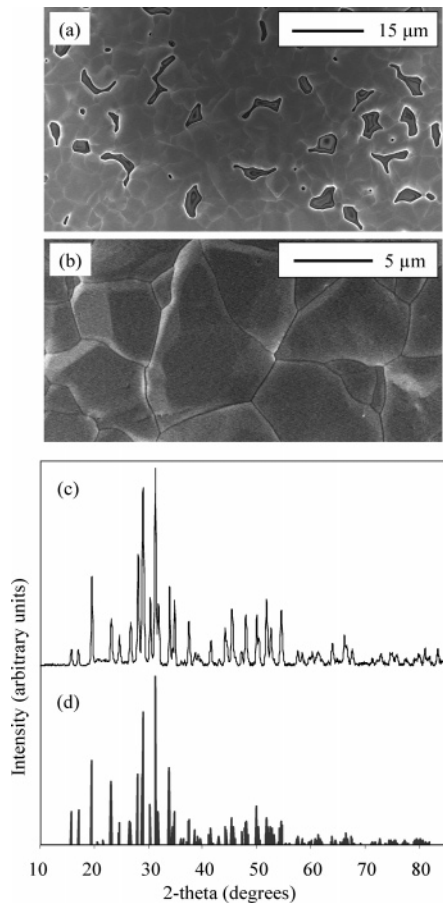


Figure 1. (a,b) SEM images of a $\text{Cu}_3\text{Bi}_3\text{S}$ film synthesized by heating a cosputtered metal precursor film at 270 °C for 16 h under 5 Torr H_2S /5 Torr Ar, (c) XRD powder pattern, and (d) standard powder pattern for $\text{Cu}_3\text{Bi}_3\text{S}$.

roughness as a consequence of the Bi top layer (Bi films exhibit faceted island growth), but were still continuous and relatively smooth with feature sizes on the order of 200 nm. XRD powder patterns identified multilayer films as being composed of crystalline bismuth and copper. Cosputtered films were found to be predominantly amorphous, as expected on the basis of the Cu–Bi binary phase diagram, which contains no stable intermetallic phases.²³

When synthesizing $\text{Cu}_3\text{Bi}_3\text{S}$ films from metal precursors, it was found that reaction conditions and precursor composition significantly impacted the morphology of the resulting film. The best results were achieved with cosputtered precursors processed at low H_2S partial pressures (5 Torr), with faster heating rates (10–20 °C/min) and long heating times (>16 h) at 270 °C. SEM images of a representative sample (1 μm thick cosputtered precursor, processed at 270 °C for 16 h with a heating rate of 10 °C/min, and 5 Torr H_2S /5 Torr Ar atmosphere) are presented in images a and b of Figure 1. The corresponding XRD powder pattern is shown in Figure 1c, along with the $\text{Cu}_3\text{Bi}_3\text{S}$ standard powder pattern (PDF 43-1479) in Figure 1d. The powder pattern confirms that the target phase $\text{Cu}_3\text{Bi}_3\text{S}$ has been synthesized and shows no extraneous peaks. These films are characterized in general by relatively smooth surfaces, large crystallites (~ 3 – $10 \mu\text{m}$ diameter), and numerous void spaces in the film.

When the optimized conditions identified above are altered, the resulting films are invariably of poorer quality.

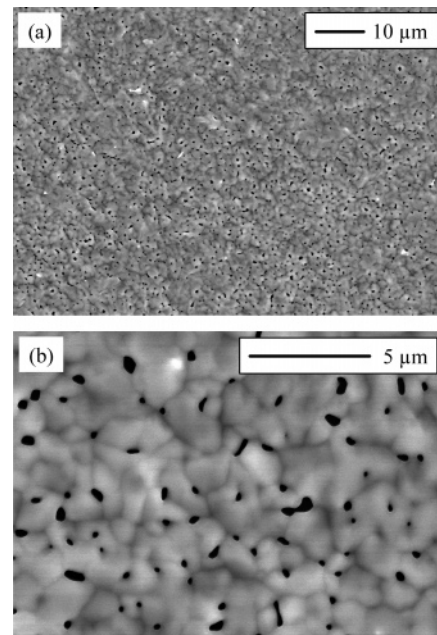


Figure 2. (a,b) SEM images of a $\text{Cu}_3\text{Bi}_3\text{S}$ film formed by heating a multilayer metal precursor film at 270 °C for 30 h under 50 Torr H_2S .

Preliminary results utilizing nonoptimized conditions were reported previously.²⁴ Specifically, if multilayer precursors, slower heating rates or higher partial pressures of H_2S are employed, the resulting films are rougher and contain an increased number of voids. This is accompanied by occasional large outgrowths randomly distributed across the surface of the film, and isolated islands containing a secondary phase ($\text{Cu}_{1.8}\text{S}$ or Bi) identified by SEM/EDX. The exact nature of the resulting film morphology is, as expected, dependent on the specifics of precursor deposition and processing with a range of suboptimum morphologies resulting. For example, presented in Figure 2 is a film formed by heating a 250 nm thick multilayer precursor at 270 °C for 30 h with a heating rate of 10 °C/minute and a 50 Torr H_2S atmosphere. When compared to the optimized morphology (Figure 1), the film is significantly rougher, the crystallites are smaller, and the film contains an increased number of voids per unit area. It should be noted that this variation cannot be attributed to variations in precursor thickness. Precursor thickness in the range of 250–1000 nm had no impact on film morphology under identical processing conditions.

When processing temperatures greater than 300 °C were employed, the resulting films were Bi depleted and of mixed composition containing both $\text{Cu}_3\text{Bi}_3\text{S}$ and Cu_2S .²⁴ When heating times less than 16 h at 250–300 °C were employed, complete conversion of the precursor did not occur and films were found to contain $\text{Cu}_{1.8}\text{S}$, Bi, and $\text{Cu}_3\text{Bi}_3\text{S}$. A backscattered electron SEM image of a partially reacted film (1 μm thick cosputtered precursor processed at 300 °C for 2 h with a heating rate of 1 °C/min and a 50 Torr H_2S atmosphere) is

(23) Baker, H., Ed. *ASM Handbooks Online*; ASM International: Materials Park, OH, 2002; Vol. 3: Alloy Phase Diagrams.

(24) Gerein, N. J.; Haber, J. A. In *Thin-Film Compound Semiconductor Photovoltaics*; Shafarman, W., Gessert, T., Niki, S., Siebentritt, S., Eds.; Material Research Society: Warrendale, PA, 2005; Vol. 865, pp F5.2.1–F5.2.6.

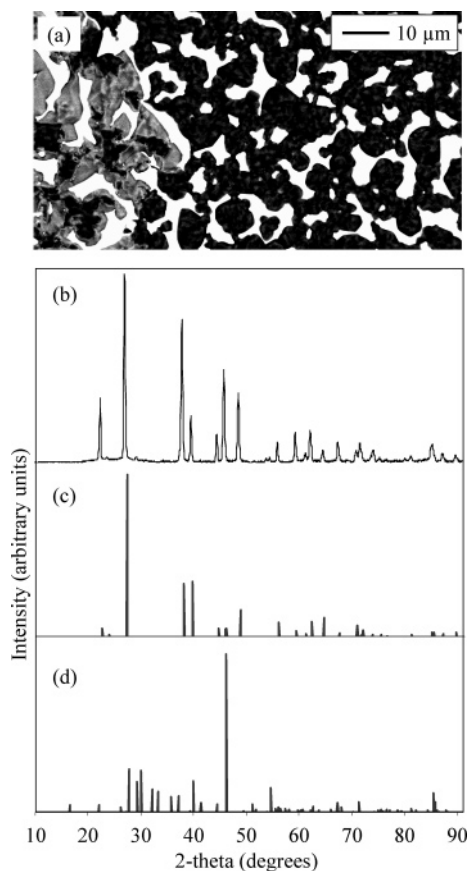


Figure 3. (a) Backscattered SEM image of a film formed by heating a cosputtered metal precursor at 300 °C for 2 h under 50 Torr H₂S with phases identified by XRD/EDX as Bi (bright areas), Cu_{1.8}S (dark areas), and by EDX as Cu₃BiS₃ (intermediate areas). (b) XRD powder pattern and standard powder pattern for (c) Bi and (d) Cu_{1.8}S are also shown.

shown in Figure 3a, along with an XRD powder pattern collected from the film and standard powder patterns for Bi (PDF 65-1215) and Cu_{1.8}S (PDF 88-2158). It should be noted that the Cu_{1.8}S standard pattern is for a rhombohedral phase (space group *R* $\bar{3}m$), which has been identified as both a stable²⁵ and metastable^{23,26} phase. Because of the weak diffraction signal from this phase, the assignment could not be made with certainty. However, the assignment is supported by the formation of the same Cu_{1.8}S phase when copper precursor films are heated under similar conditions (see below). Reports on the formation of bulk Cu_xS phases have identified the formation of rhombohedral Cu_{1.8}S above 132 ± 6 °C that persists until 262 ± 12 °C, at which point it is converted to Cu_{1.96}S.²⁶ These results are consistent with the observation of Cu_{1.8}S in this work. No diffraction from Cu₃BiS₃ was evident in the powder pattern. EDX analysis was used to confirm the identity of elemental Bi and Cu_{1.8}S phases, as well as to identify the third phase as having a composition of 3:1:3 Cu:Bi:S. The ternary phase, identified as Cu₃BiS₃, is present in much smaller amounts than the other two phases, explaining the lack of diffraction. When longer heating times are employed, the elemental Bi reacts with the intermediate Cu_{1.8}S and excess H₂S, yielding complete conversion to Cu₃BiS₃ (Figures 1 and 2).

(25) Grønvd, F.; Stølen, S.; Westrum, E. F.; Galeas, C. G. *J. Chem. Thermodyn.* **1987**, *19*, 1305–1324.

(26) Blachnik, R.; Müller, A. *Thermochim. Acta* **2000**, *361*, 31–52.

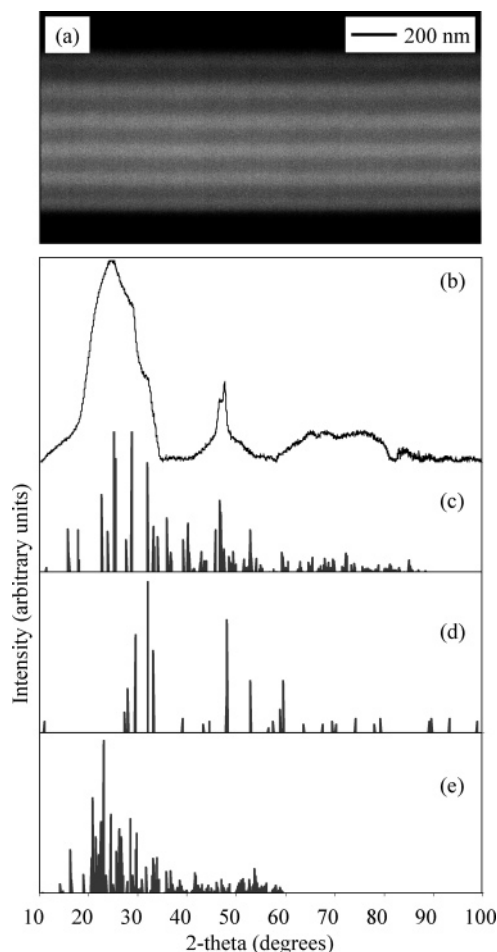


Figure 4. (a) Backscattered SEM image of a metal sulfide precursor as-deposited; bright bands are composed of Cu–Bi–S, dark bands are Cu–S. (b) XRD powder pattern and standard powder pattern for (c) Bi₂S₃, (d) CuS, and (e) S are also shown.

When metal sulfide precursors produced by sputter deposition of Cu–S and Bi are employed for the synthesis of Cu₃BiS₃, the composition of the precursor film is more complex. As in the case of cosputtered metal precursor films, the metal sulfide precursor is smooth, continuous, and mirrorlike in appearance, with no topographic contrast visible in SEM images. SEM analysis of cross-sections of precursor films shows that a multilayer structure is retained during the deposition process (Figure 4a). XRD analysis of these films suggests that a significant fraction of the film is amorphous; however, the presence of crystalline CuS, Bi₂S₃, and elemental S is also evident. The XRD powder pattern is presented in Figure 4b, along with the standard powder patterns for Bi₂S₃ (PDF 65-2435), CuS (PDF 6-0464), and S (PDF 71-0569). Diffraction from multiple phases makes phase identification difficult; however, key peaks for both Bi₂S₃ and CuS are identifiable. There is no evidence for the presence of crystalline Cu or Bi. These results suggest that when the CuS and Bi targets are sputtered simultaneously Bi₂S₃ is formed. This is thought to occur by reaction of the CuS and Bi fluxes, but could also occur by reaction of the deposited materials.

Films of single composition identical to one of the layers in the metal sulfide precursor were also prepared. WDX analysis of Cu–S films show that they are sulfur poor, with

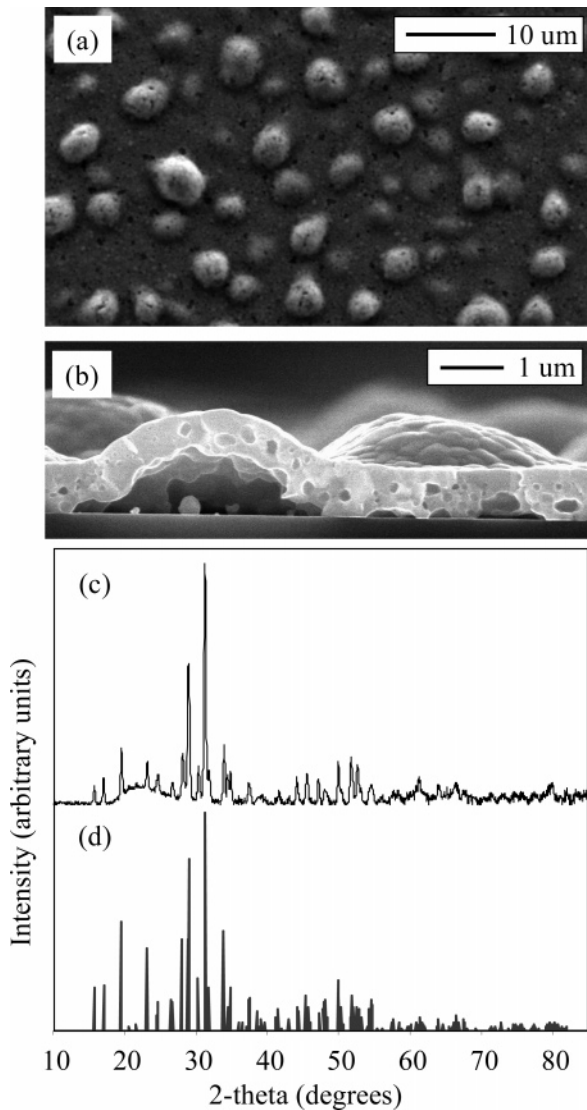


Figure 5. (a,b) SEM images of a $\text{Cu}_3\text{Bi}_3\text{S}$ film synthesized by heating a metal sulfide precursor film at 270 °C for 12 h under 5 Torr $\text{H}_2\text{S}/45$ Torr Ar, (c) XRD powder pattern, and (d) standard powder pattern for $\text{Cu}_3\text{Bi}_3\text{S}$.

a composition of 2.8:1.0 Cu:S. WDX analysis of Cu–S–Bi cosputtered films determined a composition of 1.0:3.2:1.9 Cu:S:Bi. When the metal sulfide precursor is deposited, the relative thickness of these individual layers is modulated to provide a Cu:Bi ratio of 3:1. On the basis of the WDX analysis of single-composition films, we calculated the sulfur balance in the multilayer precursor film to be 2.6 (or 3:2.6:1 Cu:S:Bi), suggesting that the as-deposited sulfide precursor film has a net sulfur deficiency, necessitating sulfurization in an H_2S atmosphere.

When metal sulfide precursors are heated in a H_2S environment, the resulting $\text{Cu}_3\text{Bi}_3\text{S}$ films are continuous, but they buckle, leaving 5–10 μm diameter round pockets between the film and the substrate. The individual crystallites are smaller than those observed in films synthesized from metal precursors. SEM images of a representative sample (metal sulfide precursor processed at 270 °C for 12 h with a heating rate of 10 °C/min and a 5 Torr $\text{H}_2\text{S}/45$ Torr Ar atmosphere) are presented in images a and b of Figure 5, along with the XRD powder pattern (Figure 5c), and standard powder pattern (Figure 5d) for $\text{Cu}_3\text{Bi}_3\text{S}$. The powder pattern

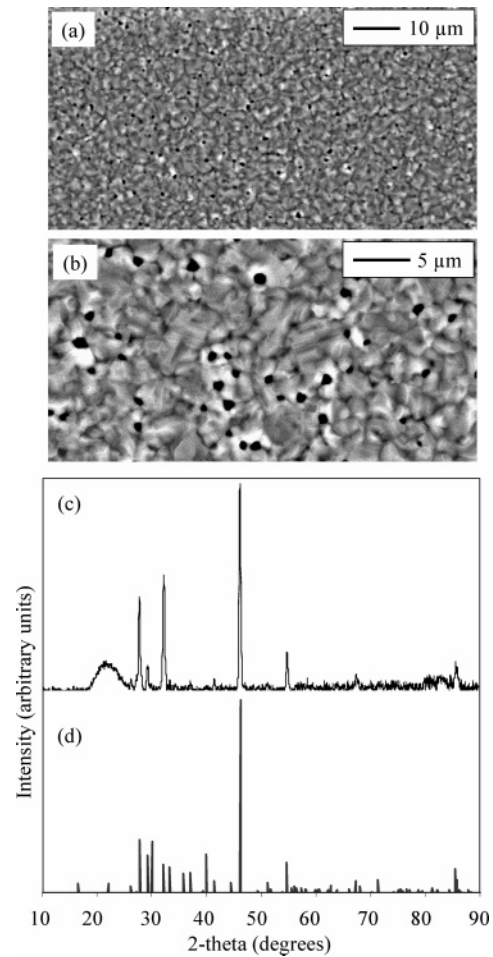


Figure 6. (a,b) SEM image of a $\text{Cu}_{1.8}\text{S}$ film formed by heating a Cu film at 250 °C for 4 h under 5 Torr $\text{H}_2\text{S}/45$ Torr Ar, (c) XRD powder pattern, and (d) $\text{Cu}_{1.8}\text{S}$ standard powder pattern.

indicates that phase-pure $\text{Cu}_3\text{Bi}_3\text{S}$ has been synthesized. This morphology was obtained regardless of H_2S partial pressure, heating rate, or processing temperature below 300 °C. Indistinguishable films could also be synthesized with heating times as short as 2 h and with H_2S partial pressures as low as 1 Torr. If temperatures greater than 300 °C were employed, it was again found that the product films were bismuth depleted.

$\text{Cu}_{1.8}\text{S}$ and Bi_2S_3 films were also synthesized via reactive annealing of Cu and Bi metal films under conditions similar to those employed for synthesis of ternary films. A SEM image of a $\text{Cu}_{1.8}\text{S}$ film (Cu precursor processed at 250 °C for 4 h with a 10 °C/minute heating rate and a 5 Torr $\text{H}_2\text{S}/45$ Torr Ar atmosphere) along with an XRD powder pattern and $\text{Cu}_{1.8}\text{S}$ standard powder pattern (PDF 88-2158) is shown in Figure 6. The powder pattern collected from the film best matches the standard powder pattern for the rhombohedral $\text{Cu}_{1.8}\text{S}$ phase also identified in the powder pattern collected from the partially reacted ternary film (Figure 3b). The morphological similarity between this film and the sub-optimum $\text{Cu}_3\text{Bi}_3\text{S}$ film synthesized from a metal precursor (Figure 2) should also be noted. The size and distribution of the voids in each film are strikingly similar. The morphological similarity of the binary and ternary film, and the XRD data from the binary film and the partially reacted film, provide evidence for the assignment of $\text{Cu}_{1.8}\text{S}$ as the

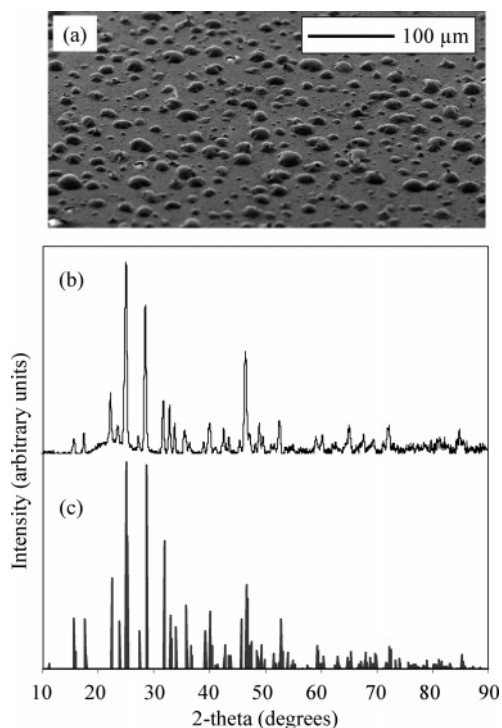


Figure 7. (a) SEM image of a Bi_2S_3 film formed by heating a Bi film at 250 °C for 12 h under 5 Torr $\text{H}_2\text{S}/45$ Torr Ar, (b) XRD powder pattern, and (c) standard powder pattern for Bi_2S_3 .

intermediate product in the synthesis of Cu_3BiS_3 from metal precursor films.

A SEM image of a Bi_2S_3 film (Bi film processed at 250 °C for 12 h with a 10 °C/minute heating rate and a 5 Torr $\text{H}_2\text{S}/45$ Torr Ar atmosphere), along with XRD powder pattern and Bi_2S_3 standard powder pattern (PDF 65-2435), is presented in Figure 7. The powder pattern confirms that Bi_2S_3 has been synthesized. In this case, the morphological similarity to the Cu_3BiS_3 film synthesized from a metal sulfide precursor (Figure 5) should be noted. The size and distribution of the pockets under each film is comparable. This morphological similarity, in conjunction with XRD data from the metal sulfide precursor film (Figure 4) and WDX data from the Cu–S–Bi film (see above), provides evidence for the formation of Bi_2S_3 during the sputter deposition process and subsequent reaction of this Bi_2S_3 intermediate with sputter-deposited Cu–S and H_2S to form Cu_3BiS_3 during annealing.

Sheet and electrical resistivity was measured on samples synthesized from both metal and metal sulfide precursors. On 1 μm thick Cu_3BiS_3 films synthesized from cosputtered metal precursors, van der Pauw resistivity measurements gave a value of $3 \times 10^4 \Omega$ for the sheet resistivity or an electrical resistivity of $3 \Omega \text{ cm}$. On 800 nm thick films synthesized from metal sulfide precursors, identical measurement methods gave a sheet resistivity of $2 \times 10^6 \Omega$ or an electrical resistivity of $2 \times 10^2 \Omega \text{ cm}$. The discrepancy in these values is attributed to the variations in film structure, thickness, and synthesis method. Crystallite dimensions and differences in defect doping as a result of differing syntheses are consistent with significant variations in electrical properties. It should be noted that within this context, these values are in reasonable agreement with the previously reported

value of $3 \times 10^1 \Omega \text{ cm}$.³ Optical transmission measurements were collected from Cu_3BiS_3 films synthesized from 250 nm thick metal precursors (see the Supporting Information, Figure S2). Qualitatively, the onset of absorbance at 850 nm is consistent with the previously reported optical band gap of 1.3 eV;³ however, significant scattering losses as a result of the poor morphology of the films limits peak transmission to $\sim 20\%$. Consequently, quantitative analysis of the optical properties of these films was not possible.

Discussion

When Cu_3BiS_3 is synthesized from metal precursors, long reaction times are required, with SEM and XRD analysis of partially converted films showing the presence of $\text{Cu}_{1.8}\text{S}$, Bi, and Cu_3BiS_3 (Figure 3). Limited diffraction signal from the rhombohedral $\text{Cu}_{1.8}\text{S}$ phase makes this identification slightly ambiguous; however, this conclusion is supported by the fact that reaction of a Cu precursor film under similar conditions results in the synthesis of a phase that is identified as $\text{Cu}_{1.8}\text{S}$, and by the fact that the reaction temperatures employed are consistent with literature reports on the formation of this phase.²⁶ We hypothesize that this $\text{Cu}_{1.8}\text{S}$ intermediate forms rapidly upon heating a Cu–Bi metal precursor in the presence of H_2S . The formation of binary sulfide intermediates has also been observed during the synthesis of CuInS_2 by heating Cu–In precursors in the presence of H_2S .⁵ The formation of Cu_3BiS_3 results from the relatively slow diffusion and reaction of Bi with the $\text{Cu}_{1.8}\text{S}$ intermediate and H_2S , a pathway that is consistent with the observed growth of large crystallites. Because of sluggish reaction at temperatures preventing volatilization of bismuth ($T \leq 300$ °C), complete reaction requires a long (16 h) heating time.

The void space that is common to all Cu_3BiS_3 films synthesized by heating metal precursors in the presence of H_2S is a consequence of the rapid formation of the copper sulfide intermediate, which possesses a discontinuous morphology similar to that observed when $\text{Cu}_{1.8}\text{S}$ is synthesized from a copper precursor film. The formation of discontinuous copper sulfide films has also been observed during the synthesis of CuInS_2 thin films.²⁷ As Bi diffuses and reacts with the $\text{Cu}_{1.8}\text{S}$ intermediate, void spaces in the film are left behind. The influence of the copper sulfide intermediate on the morphology of the final film is supported by the similarity of Cu_3BiS_3 films and $\text{Cu}_{1.8}\text{S}$ films synthesized under similar conditions (Figures 2 and 6).

This reaction pathway is also consistent with the observed effects of precursor structure (multilayer or cosputtered), heating rates, and H_2S partial pressures. Lower H_2S partial pressures are expected to decrease the rate of formation of the $\text{Cu}_{1.8}\text{S}$ intermediate. Cosputtered precursors and faster heating rates are expected to lead to increased nucleation of the ternary Cu_3BiS_3 phase. The rate of formation of the ternary phase cannot be further increased by increasing reaction temperature, as a consequence of the volatility of bismuth. A decreased rate of formation of $\text{Cu}_{1.8}\text{S}$ (lower H_2S partial pressures) and rapid nucleation of the ternary phase

(27) Scheer, R.; Klenk, R.; Klaer, J.; Luck, I. *Sol. Energy* **2004**, *77*, 777–784.

(increased heating rates and cosputtered precursors) should lead to smoother, more continuous films with decreased void space. This expectation is supported by the experimental results, with the best morphology obtained using cosputtered precursors, faster heating rates, and lower H_2S partial pressures. Qualitatively, it was found that increasing the heating rate above $10\text{ }^\circ\text{C}/\text{min}$ resulted in no appreciable improvement in film quality, whereas reducing H_2S partial pressures below 5 Torr yielded incomplete conversion of the precursor.

Studies on the selenization of Cu–In multilayer precursors under $\text{H}_2\text{Se}/\text{Ar}$ to form CuInSe_2 have also found that heating conditions have an impact on the product film morphology.²¹ Alberts and Swanepoel found that when Cu–In samples were heated to $400\text{ }^\circ\text{C}$ and then exposed to H_2Se at $400\text{ }^\circ\text{C}$ (without a temperature ramp under H_2Se), the morphology of the final film was very rough and showed some segregation of CuInSe_2 and a secondary Cu_2Se phase. They attribute this to solid–liquid phase segregation resulting from the low melting point of indium ($157\text{ }^\circ\text{C}$). When a ramp rate of $16\text{ }^\circ\text{C}$ from an initial temperature of $150\text{ }^\circ\text{C}$ under H_2Se was employed, they found that this phase segregation was avoided and film morphology improved significantly. They also report that precursor morphology directly influences product morphology.²¹ This is consistent with the observation in this work that the smoother cosputtered precursors produced product films with smoother morphology than those produced using the rougher multilayer films; however, we believe this plays a minor role in our results. Ultimately, the accessible range of processing conditions for the synthesis of $\text{Cu}_3\text{Bi}_3\text{S}$ thin films from Cu–Bi precursors, limited by the volatility of Bi above $300\text{ }^\circ\text{C}$, is not sufficient to overcome the morphology-directing influence of the pathway described above. Consequently, smooth, continuous $\text{Cu}_3\text{Bi}_3\text{S}$ films are not obtainable from metal precursor films, within the accessible parameter space of this study.

The synthesis of $\text{Cu}_3\text{Bi}_3\text{S}$ from metal sulfide precursors proceeds via a different reaction pathway from that identified for synthesis from metal precursors. XRD analysis of metal sulfide precursor films identified the presence of some crystalline CuS and Bi_2S_3 in the multilayer structure, in addition to elemental sulfur and significant amorphous content. The formation of these binary sulfides during the sputter deposition process, prior to the heating, dictates the reaction intermediates and pathway. The complete conversion of the binary sulfide intermediates formed during deposition to $\text{Cu}_3\text{Bi}_3\text{S}$ during heating occurs in a fraction of the time required for complete conversion of metal precursors. This is likely a result of the specific binary sulfide intermediates present (CuS and Bi_2S_3 vs $\text{Cu}_{1.8}\text{S}$), but may also be due to the presence of S in the precursor film, which is expected to be more reactive than H_2S . (The Gibbs standard free energy for the reaction of $\text{Cu}(\text{s})$ and $\text{H}_2\text{S}(\text{g})$ to form $\text{CuS}(\text{s})$ and $\text{H}_2(\text{g})$ is -20.2 kJ/mol , whereas the value for the reaction of $\text{Cu}(\text{s})$ and $1/2\text{S}_2(\text{g})$ to form $\text{CuS}(\text{s})$ is -93.4 kJ/mol .) At $400\text{ }^\circ\text{C}$, the Gibbs free energy for the decomposition reaction of $\text{H}_2\text{S}(\text{g})$ to $\text{H}_2(\text{g})$ and $1/2\text{S}_2(\text{g})$ is 56.9 kJ/mol ; consequently, at the maximum reaction temperatures used in this work, 1 Torr H_2S yields 7.12×10^{-4} Torr $\text{S}_2(\text{g})$, demonstrating that

a tiny amount of elemental sulfur is available during the processing of metal precursor films relative to metal sulfide precursor films. The short reaction time required (2 h) is also similar to that reported previously for the reaction of chemical bath deposited Bi_2S_3 and CuS films to form $\text{Cu}_3\text{Bi}_3\text{S}$.^{28,29}

The morphological similarity of $\text{Cu}_3\text{Bi}_3\text{S}$ films synthesized from metal sulfide precursors to Bi_2S_3 films (Figures 5 and 7) suggests that the Bi_2S_3 intermediate dictates the morphology of the $\text{Cu}_3\text{Bi}_3\text{S}$ film. The fact that this morphology cannot be controlled or even influenced by varying reaction conditions lends additional support to the hypothesis that the Bi_2S_3 forms during the deposition process and for the conclusion that the final morphology of the $\text{Cu}_3\text{Bi}_3\text{S}$ film is a function of the precursor, not the subsequent processing. We conclude that the morphology of the Bi_2S_3 film is a consequence of the incorporation of sulfur into the metal precursor during the reaction with H_2S . This produces significant volume expansion of the film, which is relieved by buckling of the film, producing pockets between the film and substrate. This reasoning also applies to the morphology of $\text{Cu}_3\text{Bi}_3\text{S}$ films synthesized via Bi_2S_3 and CuS intermediates. WDX results suggest that the as-deposited precursor is sulfur deficient. XRD shows that some crystalline Bi_2S_3 and CuS is present, but that the precursor film also has a significant amorphous component. Upon heating, the reaction of these intermediates, combined with uptake of additional sulfur, results in volume expansion of the film. In an analogous manner to the Bi_2S_3 thin film, this expansion produces buckling of the $\text{Cu}_3\text{Bi}_3\text{S}$ thin film and the formation of pockets between the film and substrate.

It has been demonstrated for the selenization of Cu–In–Ga–Se precursors that increasing the Se content in the precursor from 5 to 30 at % reduces phase segregation and enhances grain growth in the resultant $\text{Cu}(\text{In,Ga})\text{Se}_2$ films, yielding improved film morphology.³⁰ Kushiya et al. also identify reduced volume expansion during the selenization process when the Se content in the precursor is increased. Similar improvements in the morphology of CuInS_2 films heated under H_2S have been observed with increased sulfur content in the precursor film, with the improvement attributed to reduced phase segregation during processing.³¹ When our results for metal and metal sulfide precursors are compared, it appears that phase segregation during the synthesis of $\text{Cu}_3\text{Bi}_3\text{S}$ is eliminated when sulfur is incorporated into the precursor film. We attribute this to the sluggish reactivity of elemental Bi, versus the much more facile reactivity of Bi_2S_3 , with the copper sulfide intermediates.

Although we were unable to perform detailed electrical and optical characterization of these films as a consequence of the suboptimum morphology obtained in all cases, it is worth noting that electrical resistivities agree reasonably well

-
- (28) Hu, H.; Gomez-Daza, O.; Nair, P. K. *J. Mater. Res.* **1998**, *13*, 2453–2456.
(29) Nair, P. K.; Huang, L.; Nair, M. T. S.; Hu, H.; Meyers, E. A.; Zingaro, R. A. *J. Mater. Res.* **1997**, *12*, 651–656.
(30) Kushiya, K.; Shimizu, A.; Yamada, A.; Konagai, M. *Jpn. J. Appl. Phys. Part 1* **1995**, *34*, 54–60.
(31) Watanabe, T.; Matsui, M. *Jpn. J. Appl. Phys., Part 1* **1996**, *35*, 1681–1684.

with previously reported values and that the optical absorption edge is qualitatively consistent with the previously reported 1.3 eV direct band gap. In previous reports of the thin film synthesis of Cu_3BiS_3 by Nair and co-workers,^{3,29} SEM images of the films are not presented and no specific discussion of film morphology is provided. Consequently, we cannot compare the morphology of our films with those reported. On the basis of optical data presented by Nair and co-workers, it may be inferred that smoother films were obtained when Cu_3BiS_3 was synthesized from the reaction of Bi and CuS,³ rather than from the reaction of Bi_2S_3 and CuS.²⁹

Whereas synthesis of phase-pure Cu_3BiS_3 films by heating of metal and metal sulfide precursors in the presence of H_2S has been demonstrated, in both cases the morphology of the films was not suitable for use in thin film photovoltaics. On the basis of the results of our study, it is clear that although processing conditions may have an impact, the dominant factor in determining film morphology in both cases is the reaction pathway, which is directly dependent on the precursor employed. As a consequence, under the scope of the current study, we conclude that this two-step process is not applicable to the synthesis of smooth and continuous films of Cu_3BiS_3 . However, if Cu_3BiS_3 is found to show potential as a solar absorber material in thin film PV devices, these results do not preclude the use of this method for the synthesis of smooth continuous Cu_3BiS_3 films employing alternate precursors, processing conditions, or conductive substrates such as metal foils or transparent conducting oxide coated glass.

Conclusions

A physical vapor deposition technique for the synthesis of Cu_3BiS_3 has been developed, employing the heating of metal or metal sulfide precursor films under $\text{H}_2\text{S}(\text{g})$. The morphology of the final film is controlled by the binary sulfide intermediates, which are dependent on precursor

composition. Synthesis from metal precursors proceeds via formation and reaction of a discontinuous $\text{Cu}_{1.8}\text{S}$ intermediate with elemental Bi and H_2S . These films are characterized by large crystallites and voids in the film. Synthesis from metal sulfide precursors proceeds via the reaction of Bi_2S_3 and CuS intermediates formed during film deposition. These films are continuous with smaller individual crystallites; however, reaction results in volume expansion and buckling that produces pockets between the film and substrate. Although all films were phase-pure, they are not smooth and continuous—a requirement for application in thin film photovoltaics. Processing conditions have been thoroughly explored and it is not possible to overcome the controlling influence of the precursor composition and reaction pathway on film morphology. Consequently, whereas reactive annealing of Cu–In precursors under H_2S has been successfully employed for the synthesis of smooth, continuous thin films of CuInS_2 , we have determined that this method is not suitable for the production of Cu_3BiS_3 films of similar morphology on nonconductive transparent substrates. However, on the basis of our study of this process, we have developed a one-step reactive deposition for Cu_3BiS_3 that produces device quality films.²⁰

Acknowledgment. The authors acknowledge George Braybrook for collection of SEM images and EDX data, NINT for access to SEM and XRD facilities, and Sergi Matveev for collection of WDX data. Funding was provided by an NSERC-Natural Resources Canada Greenhouse Gas Mitigation Program grant (GHGP J 269903) awarded to J.A.H. N.J.G. thanks NSERC and Alberta Ingenuity for graduate studentships.

Supporting Information Available: Experimental procedure and SEM images of films on soda-lime glass, and optical transmission spectrum of a Cu_3BiS_3 film on a fused silica substrate. This material is available free of charge via the Internet at <http://pubs.acs.org>.

CM061452Z